ELSEVIER

Chemical Geology 186 (2002) 99–116

CHEMICAL GEOLOGY
INCLUDING
ISOTOPE GEOSCIENCE

www.elsevier.com/locate/chemgeo

Rb isotope dilution analyses by MC-ICPMS using Zr to correct for mass fractionation: towards improved Rb–Sr geochronology?

Tod Waight [a,*], Joel Baker [a], Bart Willigers [a,b]

[a] *Danish Lithosphere Centre, Øster Voldgade 10, L. 1350 Copenhagen K, Denmark*
[b] *Institut für Mineralogie, Universität Münster, Correnstrasse 24, 48149 Münster, Germany*

Received 17 April 2001; accepted 11 December 2001

Abstract

A new technique is presented where mass fractionation during Rb isotope dilution analyses by multi-collector inductively coupled plasma mass spectrometry is corrected for by measuring the amount of fractionation on admixed Zr. Replicate analyses of natural Rb interspersed with analyses of ^{87}Rb tracer enriched samples yield a mean $^{87}Rb/^{85}Rb = 0.38540 \pm 19$ (0.05%, 2 s.d.), assuming a natural $^{90}Zr/^{91}Zr$ of 4.588. Each Rb analysis takes 1 min, consumes 20 ng of Rb and has an internal precision of $\sim 0.02\%$ (2 s.e.). Washouts between samples take 5 min. Persistent but small stable Rb backgrounds are overcome by an on-peak-zeroes (OPZ) measurement prior to data acquisition. Close examination of measured $^{87}Rb/^{85}Rb$ and $^{90}Zr/^{91}Zr$ ratios indicate small changes in relative fractionation of Rb and Zr during plasma ionisation occur when different sample introduction techniques are used (e.g., 'wet' vs. 'dry' nebulisation), although the differences are insignificant compared to the level of precision required for isotope dilution measurements. Replicate analyses of whole rock samples suggest a reproducibility for Rb concentration measurements of $\leq 0.5\%$ and $^{87}Rb/^{86}Sr$ measurements of 0.2% when interfering Sr is reduced to satisfactory levels. However, it is difficult to ascertain to what extent this reproducibility reflects the limit of the technique or powder heterogeneity. Much of the error involved in the Rb isotope dilution and Sr isotope ratio measurements by multiple collector inductively coupled plasma mass spectrometry (MC-ICPMS) is derived from uncertainties as to which $^{87}Sr/^{86}Sr$ (and $^{87}Rb/^{85}Rb$) ratios to use when correcting for isobaric interferences due to the presence of spike Sr and Rb at mass 87. If isobaric interferences are minimised by efficient separation of Rb from Sr during cation exchange chemistry, the use of natural ratios for isobaric interference corrections yields the most reproducible data, indicating that the interferences are derived from environmental blank. Larger isobaric interferences at mass 87 are indicative of inefficient chemical separations, and the measured ratio from the complementary analysis provide more reproducible data. Burning off of Rb during conventional thermal ionisation mass spectrometry (TIMS) Sr isotope analysis nullifies this isobaric interference, and therefore, TIMS remains the method of choice for reliable and precise $^{87}Sr/^{86}Sr$ determinations on spiked samples. Application of our technique to minerals separated from Tertiary to Palaeozoic plutons yields age data consistent with previous determinations. Where different two-point isochron ages can be calculated for individual plutons, the ages reproduce to $\leq \pm 0.3\%$. The method represents an initial improvement in Rb isotope dilution measurements over TIMS by allowing a quantifiable correction to be made for mass fractionation, confirmed by duplicate analyses of standards and samples by both TIMS and MC-ICPMS. Mass fractionation corrected Rb isotope dilution analyses should result in: (1) improved Rb–Sr geochronology in examples where the

* Corresponding author. Tel.: +45-38-14-26-58; fax: +45-33-11-08-78.
E-mail address: tew@dlc.ku.dk (T. Waight).

0009-2541/02/$ - see front matter
PII: S0009-2541(01)00420-X

Rb–Sr ratio provides the largest source of error; (2) application of this improved method to Rb–Sr geochronology on smaller samples such as single mica-flakes and micro-drill samples and; (3) by comparison with other geochronological techniques, more detailed cooling and crystallisation histories of igneous and metamorphic rocks. Taking advantage of these improvements requires a reevaluation of the Rb decay constant, which this technique should also permit.

Keywords: Rb; Zr; Isotope dilution; Plasma-source mass spectrometry; Mass fractionation; Rb–Sr geochronology

1. Introduction

The alkali metal rubidium has two isotopes, ^{85}Rb and ^{87}Rb, the latter of which is radioactive and decays to ^{87}Sr with a currently accepted half-life of 48.8×10^9 a ($\lambda = 1.42 \times 10^{-11}$ a^{-1}) (Steiger and Jäger, 1977). Improved mass spectrometric techniques in the 1950s lead to the development of the Rb–Sr system as a geochronological tool that has since become arguably one of the more widely applied systems in earth sciences. Isotope dilution is the most accurate method for determination of Rb and Sr contents (and subsequently the $^{87}Rb/^{86}Sr$ ratio) for geochronology; therefore, Rb isotope ratio measurement is necessary for precise and accurate Rb–Sr geochronology. However, because Rb has only two naturally occurring isotopes, this precludes correction for mass fractionation during conventional thermal ionisation mass spectrometry (TIMS) analysis. While mass fractionation of Rb during TIMS analysis may be assessed by repeated analyses of standards, the actual reproducibility for Rb isotope dilution analyses is likely to be underestimated by this approach where the effects of other matrix elements and Rb loads of variable size are largely unconstrained. This limitation is the major source of error in attaining accurate and reproducible ages from Rb–Sr geochronology.

The advent of multiple collector inductively coupled plasma mass spectrometry (MC-ICPMS) has revolutionised isotope geosciences (e.g., Walder and Freeman, 1992; Blichert-Toft et al., 1997; Halliday et al., 1998; Yi et al., 1998; Stirling et al., 2000), particularly by enabling analysis of elements previously considered difficult or impossible by TIMS due to their high ionisation potentials (e.g., W, Hf etc.). Furthermore, simple and relatively consistent mass fractionation of elements with similar mass during plasma source ionisation enables corrections for mass fractionation in isotope systems where a stable isotope pair does not exist, by measuring fractionation in an element of similar mass. This method has been used to some success for Pb (using Tl) (Walder and Furuta, 1993; White et al., 2000), Fe (using Cu) (Anbar et al., 2000) and Cu and Zn (Maréchal et al., 1999; Zhu et al., 2000). Halliday et al. (1998) suggested that Rb could be corrected for mass bias by measuring admixed Zr. The aim of this study is to develop this technique and ascertain its reproducibility by replicate analyses of standards and samples and dating of igneous plutons of varying age. Application of this technique to determine truly accurate Rb concentrations, like any other isotope dilution technique, will depend on accurate spike calibrations, which this technique should also permit.

Recent work has suggested that using one element to correct for mass fractionation in another may be hampered by matrix effects and non-exponential mass fractionation behaviour (Thirlwall, 2000; Vance and Thirwall, 2000), however, these effects are considerably smaller than the external reproducibility required for a Rb isotope dilution analysis ($< \pm 1000$ ppm). The Rb–Zr technique has been developed for both standard solution and real rock and mineral samples at the Danish Lithosphere Centre (Copenhagen, Denmark), in collaboration with the development of Sr isotopic analysis techniques by MC-ICPMS, described in a companion paper (Waight et al., in preparation). The similar ionisation efficiencies of similar mass elements in plasma source mass spectrometry means that potential isobaric interferences (e.g., ^{87}Sr on ^{87}Rb) that can be largely ignored during TIMS analyses due to the large differences in ionisation potential, must be taken into consideration. We have developed a simple and relatively fast technique for minimising these interferences during Rb analyses, as well as correcting for them during MC-ICPMS analysis.

2. Analytical techniques

2.1. Standard and sample materials

To determine the reproducibility of the technique in determining Rb isotope ratios, replicate analyses were made on mixed Rb–Zr standard solutions made up to ca. 200 ppb each in 0.2% HNO_3 from stock solutions prepared from 1000 μg/ml Alfa Aesar Specpure® plasma standard solutions of $ZrCl_2O$ and Rb_2CO_3. Stock solutions of Rb and Zr are in dilute HNO_3 and HCl, respectively. We have found that the relative strength of signals from mixed stock Rb–Zr solutions varied over a period of several months due to the difficulty of keeping Zr in solution in HNO_3, however, this has no effect on the relative fractionation or isotopic composition of the two elements.

To test the Rb isotope dilution by MC-ICPMS method on real geological materials, we chose to analyse in replicate three rock powders and SRM607, with a range in Rb–Sr ratios of 0.03–13.3. The rock powders are of fine grained volcanics from Yemen, which are hopefully homogenous with respect to a typical sample size analysed (100 mg). We also constructed Rb–Sr mineral isochrons for a series of intrusions with well-known and poorly constrained ages, ranging from Proterozoic to Tertiary. Brief descriptions of the intrusions and previous age determinations are presented in Table 1. Apatite from Jabal Hufash pluton was separated by centrifuging a heavy, non-magnetic fraction in sodium polytungstate. All other mineral samples were handpicked from either coarsely crushed or sieved samples of whole rocks or, in some cases, directly from the whole rock sample itself.

Table 1
Description of samples chosen for geochronological investigations in this study and previous age determinations

Intrusive complex	Previous age determinations	Method	Details
Jabal Hufash granite (Central Yemen)	21.9 ± 0.7 Ma[9] 22.2 ± 0.8 Ma[9] 25 ± 13 Ma[10] 25 ± 13 Ma[10]	K–Ar whole rock K–Ar whole rock Rb–Sr w.r. Rb–Sr w.r.	A-type granite intruding Oligocene flood basalts, comprises alkali feldspar, quartz, alkali amphibole, zircon, fluorite, magnetite and apatite. Cross cutting relationships with dated units and $^{40}Ar-^{39}Ar$ ages on coeval rhyolites indicate the pluton must be between 29 and 26 Ma in age (Baker et al., 1996a). $^{87}Sr/^{86}Sr_i = 0.7058-0.7137$ (see also Tommasini et al., 1994; Baker et al., 1996b).
Gardiner complex (East Greenland)	ca. 50 Ma[6] 54.4 ± 0.2 Ma[7] 54.3 ± 1.1 Ma[8]	apatite fission track $^{40}Ar-^{39}Ar$ phlogopite apatite–eudialyte Lu–Hf	Pegmatite dike comprising apatite, biotite and pyroxene. $^{87}Sr/^{86}Sr_i$ = ca. 0.7037 (see also Nielsen, 1981; Nielsen and Buchardt, 1985; Nielsen and Holm, 1993; Nielsen et al., 1997)
Khibina complex, Kola alkaline province (Russia)	365.9 ± 5.9 Ma[5] 377.3 ± 3.9 Ma[5]	Rb–Sr w.r.–mineral Rb–Sr w.r.–mineral	Coarse grained biotite-bearing apatite from the centre of the intrusion. Biotite is zoned with a pale-green core and a distinct brown rim. $^{87}Sr/^{86}Sr_i = 0.7038-0.7041$.
Gouldsboro granite, Coastal Maine magmatic province (USA)	ca. 420 Ma[4]	$^{40}Ar-^{39}Ar$ on nearby related plutons	Part of a bimodal suite of plutons. Sample is a biotite–hornblende granodiorite, $^{87}Sr/^{86}Sr_i = 0.7051-0.7054$ (Waight, unpublished data) (see also Wiebe and Adams, 1997; Wiebe and Ulrich, 1997).
Illimaussaq complex, Gardiner igneous province (southern Greenland)	1143 ± 20 Ma[1] 1130 ± 50 Ma[2] 1160 ± 5 Ma[3]	Rb–Sr w.r.–mineral Sm–Nd w.r.–mineral U–Pb baddeleyite	Alkali feldspar–eudialyte bearing cumulate from latter stages of the intrusion, typified by relatively radiogenic $^{87}Sr/^{86}Sr_i$ (see also Bailey et al., 1981; Upton and Emeleus, 1987; Stevenson et al., 1997)

References: (1) Blaxland et al. (1976), (2) Paslick et al. (1993), (3) G. Markl (personal communication), (4) R.A. Wiebe (personal communication), (5) Kramm et al. (1993), (6) Gleadow and Brooks (1979), (7) C. Tegner (personal communication), (8) G. Hoffmann Barford (personal communication), (9) Capaldi et al. (1987) and (10) Coleman et al. (1992).

2.2. Chemistry

Prior to sample dissolution, mineral samples were washed several times in Milli-Q water to remove any adhering foreign matter. In addition, mica samples were also rinsed for a few minutes in cold 2.5 M HCl to remove adhering and/or included apatite grains. Samples were then weighed into Savillex™ PFA vials. Silicate rock and mineral samples were spiked with a mixed $^{84}Sr-^{87}Rb$ tracer and dissolved using conventional $HF-HNO_3-HCl$ dissolution techniques. Three separate mixed spikes were used, constructed from ca. 81% enriched ^{84}Sr and ca. 97% enriched ^{87}Rb, with Rb–Sr ratios of ca. 0.02, 0.1 and 30. The Rb isotopic composition of the spike ($^{87}Rb/^{85}Rb = 34.9284$) was determined by MC-ICPMS using the same admixed Zr solution to ensure internal consistency within the data set. Providing samples are appropriately spiked, small errors in the isotopic composition of the spike have little effect on concentration determinations. Spikes were calibrated using a combination of mixed gravimetric Rb–Sr solutions and international standards such as SRM607. The good agreement between our ID concentration data on previously analysed samples and international standards (see Table 3) gives us confidence that our spikes are indeed well calibrated. However, improvements in spike calibration in light of the technique developed here will allow for significantly more accurate Rb concentration determinations than hitherto possible.

Apatite and eudialyte were dissolved using HCl and analysed unspiked, assuming $Rb/Sr = 0$. Rb and Sr were initially separated on conventional cation exchange columns loaded with AG50W-X 100–200 mesh resin by elution of 2.5 M HCl. In order to minimise isobaric interferences on ^{87}Rb from ^{87}Sr, the resulting Rb cut was evaporated and redissolved in 3M HNO_3. This was then loaded onto miniature Teflon columns loaded with Sr-Spec resin and several reservoir volumes of 3M HNO_3 containing Rb were collected, with any Sr left from the primary cation exchange columns remaining on the Sr-Spec resin. Sr samples were also further purified using Sr-Spec resin. In most cases, this technique resulted in Rb fractions with only small Sr interferences ($^{87}Rb/^{87}Sr < 0.01$) that could easily be corrected for using the on-line software. Full procedural blanks for this technique amounted to less than 50 pg of Rb and Sr.

2.3. Sample introduction

Samples were analysed using a VG Axiom MC-ICPMS, a double-focussing magnetic sector ICPMS, located at the Danish Lithosphere Centre. Prior to analysis, samples were evaporated and redissolved in 0.2% HNO_3 doped with 200 ppb Zr, with the aim of achieving signals of 2–4 V on the largest Rb isotope, and ≥ 2 V on ^{90}Zr. A distinct advantage of MC-ICPMS is that it is possible to standardise the strength of the analyte solution, ensuring similar signal strengths and amounts of sample consumed. During the initial stages of this project, samples were introduced into the mass spectrometer using a Cetac Aridus microconcentric desolvating nebuliser, which yields excellent sensitivity for Rb (ca. 120 V of total signal per parts per million of Rb in solution). Subsequently, sample introduction was carried out using a lower sensitivity (20–30 V/ppm) Micromist nebuliser (uptake rate of 0.1 ml/min). With this sample introduction technique, solutions pass through a glass nebuliser directly into a jacketed, water-cooled spray chamber prior to entering the Ar plasma. Solutions can either be introduced into the spray chamber by free-aspiration, or pumped into the nebuliser using a peristaltic pump, where a section of Tygon tubing is attached to the Teflon uptake tube. For Rb, we chose to use the latter technique with a pumping speed of 4%. Ar is used as both the carrier and nebuliser gas and typical gas flow settings were 0.9 l/min (nebuliser), 1.1 l/min (auxiliary) and 14.0 l/min (cool).

Fast washouts were possible using the Micromist nebulisers, and were carried out by pumping 2% HNO_3 through the system for ca. 5 min. However, Rb remains difficult to fully washout from the introduction system and stable background signals of up to 1–3 mV of ^{85}Rb typically remain even after protracted washout times (several hours). This background would slowly rise by 1–2 mV during continuous periods (several days) of Rb (or Sr) analysis. Analysis of this background signal indicated that it was significantly enriched in ^{87}Rb, indicating it is an accumulation of both natural Rb and ^{87}Rb-enriched isotope dilution samples. Replacement of Tygon tubing on the peristaltic pump revealed that this was not the source of the background signals. Instead, moving the ICP torch closer to the skimmer cones, or decreas-

ing the auxiliary gas flow thereby increasing the temperature at the end of the torch, resulted in large (>100 fold) but temporary increases in Rb background, which returns to lower than the previously ambient levels when normal torch and gas flows are restored. This suggests that the background Rb is associated with slow but progressive build-up of Rb (and Sr) on the torch and cones during the course of several days of analysis. Removal and cleaning of the entire introduction system (torch, spray chamber, nebuliser, tubing and fittings) in concentrated HNO_3, and fitting of clean cones entirely removes background Rb signals, confirming this observation. As such, regular cleaning of torch and cones is necessary to obtain satisfactory Rb background levels. No evidence is observed for build up of Rb or Sr on the transfer lens stack.

2.4. Mass spectrometry

At the time of this work, the Axiom MC-ICPMS was equipped with one fixed and eight movable Faraday collectors, with 10^{11} Ω resistors on all channels. The Faraday cup set-up used for Rb is the same as that we use for Sr with an array from ^{83}Kr (L4) to ^{91}Zr (H4) (^{87}Sr and ^{87}Rb in the Axial cup), monitoring Kr, Rb, Sr, Y and Zr. Prior to analysis, collectors are aligned using a tuning solution containing Rb, Sr and Zr; Kr is aligned by allowing the instrument to aspirate atmospheric Kr. The main source of Kr is from the Ar gas, and is generally very low. However, occasional tanks of Ar have relatively high Kr levels and effectively make Rb and Sr analysis impossible. A similar problem is also occasionally encountered as Ar tanks become depleted and the heavier noble gases become enriched with respect to Ar. Relative gains on the Faraday collectors are measured once the instrument has reached thermal stability, and remeasured if the bench temperature changes by more than 1 °C, although relative changes in gains are insignificant (<50 ppm) compared to the levels of reproducibility required in this study (<1000 ppm). Cup efficiencies on the Axiom are stable and are generally not changed over long periods (weeks) of analysis. While the Axiom MC-ICPMS is capable of high mass resolution measurements (up to 13 000), all Rb isotopic measurements are carried out at low mass resolution (400) in static mode.

2.5. Data acquisition and reduction

In order to account for stable Rb backgrounds from the torch and cones, an on-peak-zeroes (OPZ) measurement is made prior to the onset of analysis. Following washout to stable background signals (ca. 1–2 mV ^{85}Rb), the sample introduction system is equilibrated and stabilised using a solution of the exact same molarity as that used to dilute samples (0.2% HNO_3). The intensity of these backgrounds are then measured on-mass for a period of 1 min. Following this, the background signal is again monitored visually to ensure it has not drifted or become unstable during the OPZ measurement. On rare occasions, the background was observed to have changed due to insufficient washing prior to starting the analysis, in these cases the analysis is stopped and the cleaning procedure repeated. Once stable background signals are achieved the uptake tube is then transferred into the sample solution and once a steady signal is achieved, collection of data begins. The background signals from the OPZ measurement are subsequently subtracted on-line from the measured signals. This effectively cancels out background signals from incomplete washouts, as these backgrounds do not change over the relatively short duration of the analysis.

Data are collected as a single block of 60 1-s measurements, if it is suspected that the background is changing during the course of the analysis, individual ratios can be monitored for signs of drift. A typical Rb isotope dilution analysis carried out in this fashion consumes ca. 0.1 ml of solution (ca. 20 ng of Rb) and lasts 2–3 min (including OPZ measurement and wash-in time), followed by 3–5 min of washout, enabling a relatively rapid throughput of samples (ca. 10 samples/h).

Most data manipulation (fractionation correction, interference corrections, etc.) is carried out on-line, and can be modified at any time during or after the analysis. Rb concentrations are determined offline. The isobaric interference of Sr on Rb at mass 87 is corrected by monitoring mass ^{88}Sr and a user specified ^{87}Sr/^{86}Sr composition, fractionated using the ^{90}Zr/^{91}Zr ratio as described below. As discussed in more detail later, a natural Sr ratio of 0.71 is applicable providing the isobaric Sr interference is relatively low (^{87}Sr/^{87}Rb>1%). A two stage column se-

paration chemistry using traditional cation exchange columns followed by Sr-specific resin greatly reduces the abundance of interfering Sr, generally making such corrections minor, especially in moderate to high Rb–Sr samples.

The $^{87}Rb/^{85}Rb$ ratio (corrected for isobaric ^{87}Sr) is then exponentially fractionation corrected using the following expression:

$$\frac{^{87}Rb}{^{85}Rb}\text{frac.corr.} = \frac{^{87}Rb}{^{85}Rb}\text{meas.} \Big/ \left(\frac{^{90}Zr/^{91}Zr_{meas.}}{4.5882}\right)^{\frac{\ln(\text{mass}^{87}Rb/\text{mass}^{85}Rb)}{\ln(\text{mass}^{90}Zr/\text{mass}^{91}Zr)}}.$$

Mass fractionation varies between 0.8% and 1.2% per a.m.u. and is dependant on the exact set-up of the machine, especially torch tuning parameters and gas flows. The mass fractionation is generally relatively stable once the instrument has reached a stable operating temperature and providing tuning conditions are not drastically changed. On individual days of analysis the mass fractionation (i.e., $^{90}Zr/^{91}Zr$ measured/real) varied by up to 0.1%.

It is beyond the scope of this paper to discuss the real isotopic composition of Zr. However, the $^{90}Zr/^{91}Zr$ value we have chosen in this study is within the range of those presented by Sahoo and Masuda (1997) ($^{90}Zr/^{91}Zr = 4.5874 \pm 74$; 2 s.d.) and in good agreement with those of Minster and Ricard (1981) and Sanloup et al. (2000) (all Zr isotope data normalised to $^{94}Zr/^{90}Zr = 0.3381$). Extrapolating the variation in natural $^{90}Zr/^{91}Zr$ measured by Sahoo and Masuda (1997) into a typical natural Rb analysis results in variations in the fractionation-corrected Rb composition of $\pm 0.04\%$, less than our external reproducibility. Hirata and Yamaguchi (1999) used a $^{90}Zr/^{91}Zr$ value of 4.5842 as a normalisation value during Zr isotopic studies based on a work by Nomura et al. (1983). Use of this value in our Rb isotope dilution analyses would result in an upward shift in the absolute isotope ratio. However, the shift would result in no change in our data reproducibility, which is the principle objective of this study. As all our standards, samples and spike compositions were determined using the same Zr isotopic composition, the actual choice of Zr isotopic composition has no bearing on the reproducibility of our data.

3. Results

3.1. Standard solutions

Replicate analyses ($n = 45$) of a ~200 ppb Rb solution doped with 200 ppb Zr, carried out over two periods in July and August 2000, yield a reproducibility for fractionation corrected $^{87}Rb/^{85}Rb$ of 0.38540 ± 19 (0.049%; 2 s.d.) (Fig. 1). The external reproducibility is only ca. three times greater than the typical internal precision (0.02%, 2 s.e.) of the analyses. Previous standard solutions analysed using the Aridus desolvating nebuliser (and prior to the onset of OPZ) yield a similar reproducibility of $^{87}Rb/^{85}Rb = 0.38555 \pm 16$ (2 s.d.) (data not presented here). Experiments have shown that internal precision increase systematically with decreasing Zr content (and therefore increasing error on measured $^{90}Zr/^{91}Zr$, which propagates into the mass fractionation correction). Our studies indicate that a Zr–Rb ratio of 1–4 is optimal, and that no effect on the mass fractionation corrected Rb ratio was observed at the levels of precision sought in this study by varying the Rb–Zr ratio by at least an order of magnitude (data not shown). A small difference in average $^{87}Rb/^{85}Rb$ is observed between data collected over two separate periods of analysis (July and August 2000), which used slightly different sample introduction systems (Micromist 50 and 100 μl/min) (Fig. 1), although the averages are the same within error. External reproducibility for these two separate analysis periods (0.039%, 2 s.d.) is slightly better than for the data set as a whole. It is important to note that all these standard analyses were performed under real operating conditions, i.e., interspersed with isotope dilution analyses of rocks and minerals with $^{87}Rb/^{85}Rb$ ratios ranging from 0.5 to 23. The well-constrained reproducibility of the standard data demonstrates the efficiency of the on-peak-zeroes procedure in counteracting small (0.1%) background signals with enriched and slowly changing Rb isotopic compositions.

3.2. Comparison with thermal ionisation mass spectrometry

As a test to compare Rb analyses by MC-ICPMS and TIMS, the parental 1000 ppm Rb standard sol-

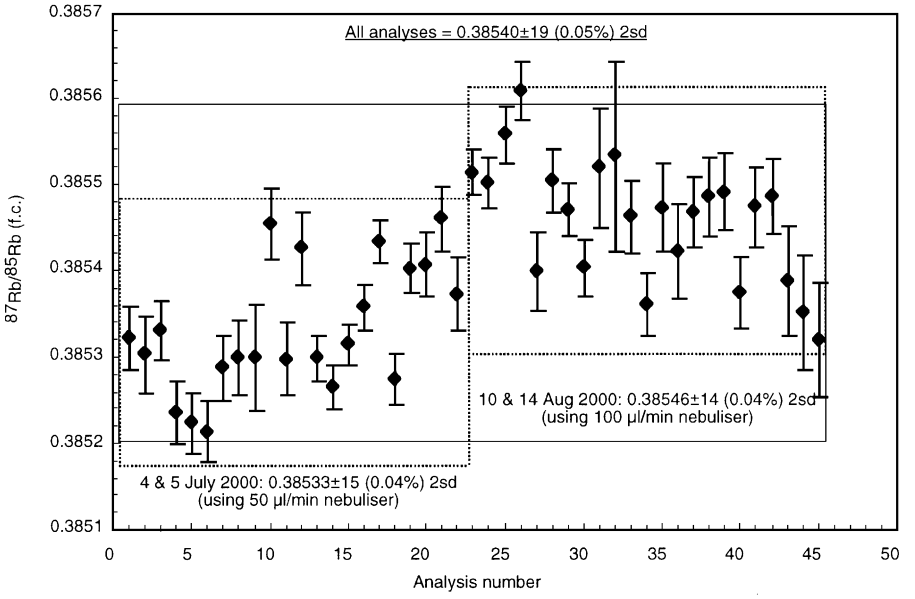

Fig. 1. Replicate analyses of standard solutions of natural Rb doped with Zr to monitor mass fractionation. Individual errors are the internal precision (2 s.e.) from each analysis.

ution used in the above experiments was analysed (without Zr) in replicate on a VG Sector 54 TIMS at the Geological Institute, University of Copenhagen. Approximately 2 μg of Rb was loaded onto a Ta side filament in a triple Ta–Re filament assembly. Twelve individual standards were loaded and run twice on consecutive days. Each sample was heated identically to 1100 °C using an automated warm-up routine followed by an automated focussing routine. Rb was then analysed as a static routine as 2 blocks of 20 × 1-s measurements. This experiment yielded an average fractionation uncorrected value of $^{87}Rb/^{85}Rb = 0.38346 \pm 0.00025$ (0.07%, 2 s.d.; $n = 22$; Fig. 2), somewhat worse than that achieved by MC-ICPMS. However, this average value excludes two analyses, one which yielded a value of $^{87}Rb/^{85}Rb = 0.3962$ on its second analysis (despite giving a value of 0.3836 during its first run), and a second sample which was analysed after having been left at running temperatures for 1 h to yield $^{87}Rb/^{85}Rb = 0.3854$ (previously gave 0.3832). This same standard that ran again the next day yielded a more typical $^{87}Rb/^{85}Rb$ of 0.3836. Inclusion of these two outlying analyses is justifiable due to the large sample sizes and consistent running conditions and yields a much poorer reproducibility of $^{87}Rb/^{85}Rb = 0.38405 \pm 0.00514$ (1.3%, 2 s.d.; $n = 25$; Fig. 2). The average TIMS standard value yielded by this experiment is ca. 0.6% lower than the fractionation corrected value determined by MC-ICPMS, this discrepancy is the result of the relatively large quantities of Rb loaded and the TIMS data not being corrected for mass fractionation and preferential ionisation of the light Rb isotope during analysis.

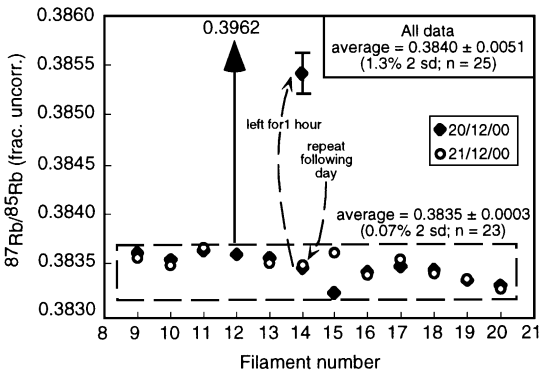

Fig. 2. Plot of $^{87}Rb/^{85}Rb$ data collected using TIMS on 12 separate loads (ca. 2 μg each) of Rb standard solution. Data collected on two consecutive days are indicated by the different symbols.

Table 2
Comparative analyses of Rb isotope dilution cuts from mineral samples (spiked using a mixed $^{85}Rb-^{84}Sr$ spike) carried out both by single collector TIMS at the University of Münster and MC-ICPMS at the Danish Lithosphere Centre

Sample	TIMS $^{87}Rb/^{85}Rb$	MC-ICPMS $^{87}Rb/^{85}Rb$	Percent deviation of TIMS from MC-ICPMS
xx-Pol-3	0.5611	0.5640	− 0.5194
xx-Pol-4	0.5101	0.5119	− 0.3691
86035-Bio-4	0.5889	0.5908	− 0.3265
431283-bio-3	0.9968	0.9991	− 0.2299
86035-Bio-2	0.6782	0.6790	− 0.1215
10812	0.8736	0.8728	− 0.0960
10822	48.8257	48.8456	− 0.0407
86035-Bio-5	0.5879	0.5881	− 0.0401
Phlogopite-4	1.6262	1.6268	− 0.0352
448975-phl	0.8869	0.8871	− 0.0216
86035-Bio-3	0.5549	0.5549	− 0.0014
Phlogopite-1	1.1922	1.1919	0.0191
449178-phl	1.2593	1.2589	0.0327
Phlogopite-3	1.5764	1.5758	0.0356
spk/spl mix 9	1.5910	1.5902	0.0543
10811	1.3725	1.3717	0.0650
449141-ms	0.8068	0.8062	0.0822
449056-bio	0.6298	0.6292	0.0882
10814	3.3808	3.3769	0.1137
spk/spl mix 6	2.0582	2.0552	0.1444
10813	4.8397	4.8302	0.1961
430603-bio	0.6083	0.6070	0.2093
448962-phl	0.6582	0.6567	0.2261
431283-bio-2	1.0439	1.0415	0.2300
449041-bio	0.5067	0.5055	0.2418
449186-bio	0.6224	0.6209	0.2502
449041-ms	0.5574	0.5559	0.2752
415528-ms	1.1536	1.1504	0.2827
415528-bio	0.7898	0.7875	0.2893
10820	49.0364	48.8492	0.3833
449186-ms	0.6829	0.6802	0.3962
449186-plag	0.4338	0.4319	0.4551
spk/spl mix 5	2.1893	2.1791	0.4700

Natural Rb standards run during the acquisition of these data yield $^{87}Rb/^{85}Rb = 0.3833 \pm 12$ (0.3% 2 s.d., $n = 29$; single collector TIMS) and 0.3855 ± 2 (0.06% 2 s.d., $n = 16$; MC-ICPMS). Several outliers (with percent deviations of -12 to $+35\%$) are excluded and are likely a consequence of over-spiking.

In reality, this experiment is likely an inaccurate reflection of Rb analytical reproducibility by TIMS. Real rock samples will contain variable, and often less Rb than loaded here, and also contain other matrix elements (Ba, K and Na), which will result in less consistent sample to sample fractionation. Differing filament currents will be needed to achieve acceptable beam sizes and also resulting in variable mass fractionation. Even with the relatively large amounts of Rb loaded in this experiment, especially compared to that consumed by a typical MC-ICPMS analysis (2 μg vs. 20 ng), it is apparent that it is easy to cause variable and unpredictable mass fractionation by TIMS even without varying the heating routine and running conditions.

As a more accurate test of the MC-ICPMS technique versus conventional TIMS Rb isotope dilution analyses, a series of Rb isotope dilution cuts from mineral separates (part of a separate Rb–Sr geochronology study) were analysed both by single collector TIMS at the University of Münster (loaded on single Ta filaments) and by MC-ICPMS in Copenhagen (Table 2). The TIMS data reveal varying degrees of deviation from the MC-ICPMS data and suggest that the TIMS Rb isotope dilution data may vary by $\pm 0.5\%$ as a consequence of variable mass fractionation due to differing amounts of Rb and other elements present during TIMS analyses (Fig. 3). The TIMS data (Fig. 3 and Table 2) clearly show that it is difficult to ascribe reproducibilities on measured Rb ratios and concentration determinations by TIMS even by replicate analyses of natural standards, where load sizes are large and matrix effects and running conditions are uniform. The offset in the median of the deviation of TIMS from MC-ICPMS data may simply be a consequence of the chosen value of the Zr isotope ratio used.

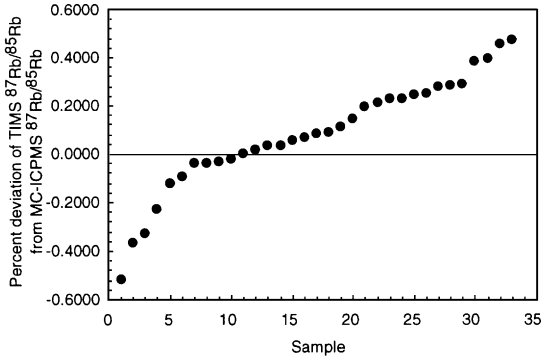

Fig. 3. Plot illustrating relative deviation of TIMS Rb analyses from MC-ICPMS analyses of the same spiked mineral separates.

Table 3
Replicate analyses of SRM607 and three whole rock volcanic samples, previously analysed by long-counting time XRF spectrometry at Royal Holloway University of London (Baker, 1996)

Sample	$^{87}Sr/^{87}Rb$ interference Rb analysis	$^{87}Rb/^{87}Sr$ interference Sr analysis	Rb (ppm) $^{87}Sr/^{86}Sr$ measured	Rb (ppm) $^{87}Sr/^{86}Sr$ 0.7100	Sr (ppm) $^{87}Rb/^{85}Rb$ measured	Sr (ppm) $^{87}Rb/^{85}Rb$ 0.3855	Rb/Sr using measured corrections	Rb/Sr using natural corrections	$^{87}Sr/^{86}Sr$ using measured Rb	$^{87}Sr/^{86}Sr$ using Natural Rb
NYJB140a	0.0924	0.0004	*33.76*	*33.83*	*1087.4*	*1087.4*	0.03104	0.03111	0.703780	0.703900
NYJB140b	0.0169	0.0002	34.15	34.16	1105.2	1105.2	0.03090	0.03091	0.703868	0.703924
NYJB140c	0.0110	0.0000	34.31	34.32	1105.2	1105.2	0.03104	0.03105	0.704001	0.703945
NYJB140d	0.0216	0.0001	34.21	34.23	1102.6	1102.6	0.03103	0.03104	0.703854	0.703896
NYJB140e	0.0748	0.0000	34.19	34.25	1102.4	1102.4	0.03101	0.03107	0.703908	0.703902
NYJB140f	0.1099	0.0001	34.15	34.24	1106.0	1106.0	0.03088	0.03095	0.703889	0.703920
Average			34.20	34.24	1104.3	1104.3	0.03098	0.03102	0.703883	0.703915
1 s.d.			0.07	0.06	1.66	1.66	0.00008	0.00008	0.000072	0.000019
2 s.d.%			0.39	0.33	0.30	0.30	0.487	0.488	0.021	0.005
NYJB140-RHULxrf				34.2		1104.3		0.03097		0.70391
NYJB271a	0.0010	0.0012	58.35	58.35	391.57	391.59	0.14902	0.14901	0.705856	0.706259
NYJB271b	0.0076	0.0007	58.37	58.38	392.61	392.62	0.14867	0.14868	0.706265	0.706496
NYJB271c	0.0010	0.0015	58.03	58.03	390.07	390.09	0.14876	0.14875	0.705752	0.706270
NYJB271d	0.0000	0.0003	58.16	58.16	391.29	391.29	0.14864	0.14864	0.706194	0.706282
NYJB271e	0.0005	0.0012	58.19	58.19	391.10	391.12	0.14879	0.14879	0.705921	0.706287
Average			58.22	58.22	391.33	391.34	0.14878	0.14877	0.706000	0.706319
1 s.d.			0.14	0.14	0.91	0.91	0.00015	0.00014	0.000222	0.000099
2 s.d.%			0.49	0.49	0.47	0.47	0.201	0.194	0.063	0.028
NYJB271-RHULxrf				58.3		391.7		0.14884		0.70622
NYJB232a	0.0000	0.0004	178.24	178.24	13.35	13.35	13.3509	13.3509	0.720995	0.721258
NYJB232b	0.0000	0.0014	177.76	177.76	13.29	13.29	13.3726	13.3746	0.729848	0.728824
NYJB232c	0.0000	0.0185	177.84	177.84	13.29	13.30	13.3824	13.3673	0.718062	0.729581
NYJB232d	0.0000	0.0031	177.79	177.79	13.31	13.31	13.3568	13.3548	0.719818	0.721730
NYJB232e	0.0000	0.0024	177.87	177.87	13.33	13.33	13.3427	13.3407	0.719749	0.721273
Average			177.90	177.90	13.32	13.32	13.3611	13.3577	0.721694	0.724533
1 s.d.			0.19	0.19	0.03	0.02	0.0162	0.0135	0.004676	0.004275
2 s.d.%			0.22	0.22	0.39	0.35	0.242	0.201	1.296	1.180
NYJB232-RHULid				177.9		12.45		14.2892		0.72102
SRM607a	0.0026	0.0001	527.15	527.13	65.67	65.68	8.02672	8.02614	1.200005	1.200316
SRM607b	0.0288	0.0007	522.95	522.74	65.38	65.40	7.99824	7.99284	1.199277	1.202186
SRM607c	0.0006	0.0040	523.98	523.97	65.45	65.47	8.00639	8.00351	1.201700	1.205372
Average			524.69	524.61	65.50	65.52	8.01045	8.00750	1.200327	1.202625
1 s.d.			2.19	2.26	0.15	0.14	0.01467	0.01700	0.001243	0.002556
2 s.d.%			0.83	0.86	0.47	0.44	0.366	0.425	0.207	0.425
Recommended				523.9 ± 1.01		65.49 ± 0.32		8.00030		1.20039 ± 20

Relatively low concentration determinations for NYJB140a (in italics) are not included in averages and likely represent substantial weighing errors.

3.3. Reproducibility of Rb concentrations and Rb–Sr ratios in homogeneous samples

In order to test the reproducibility of our method on geological materials, we undertook replicate analyses of three whole rock samples with variable Rb–Sr ratios and contents, and the NBS feldspar standard SRM607 (Table 3). The whole rock samples (Oligocene basalt, andesite and rhyolite volcanics from Yemen) have previously been analysed for Rb and Sr by high quality, long counting period XRF, or TIMS isotope dilution at Royal Holloway University of London (Baker, 1996).

User-specified $^{87}Sr/^{86}Sr$ and $^{87}Rb/^{85}Rb$ ratios are required to calculate the number of ^{87}Sr counts interfering on ^{87}Rb during the Rb isotope dilution analysis (and vice versa) prior to calculating Rb and Sr concentrations and spike corrected Sr isotope ratios. The ratio used can be either ''natural'' values (i.e., $^{87}Sr/^{86}Sr = 0.71$ and $^{87}Rb/^{85}Rb = 0.3855$) or the isotopic composition measured during the complementary analysis on the sample–spike mixture (i.e., enriched in ^{87}Rb and ^{86}Sr), depending on what the analyst believes is the source of the isobaric interference. The replicate analyses presented in Table 3 have concentration and ratio data presented using both natural and measured compositions to correct for isobaric interferences, and in most cases the different values result in only small changes in measured Rb and Sr concentrations and Rb–Sr ratio, but they do result in significant changes in the measured $^{87}Sr/^{86}Sr$ ratio. Replicate Rb and Sr concentration determinations on the Yemen rock samples with highly variable Rb–Sr ratios and Rb and Sr contents reproduce to $< 0.5\%$ (2 s.d.). Rb–Sr ratios reproduce to ca. 0.2% in the moderate and high Rb/Sr samples, but reproduce somewhat more poorly in the case of the low Rb/Sr sample ($\pm 0.5\%$). Much of this variability appears to be a consequence of high interferences ($^{87}Sr/^{87}Rb > 1\%$) during the Rb analysis of this low Rb/Sr sample, but may also represent some sample heterogeneity. Reproducibility of Sr concentration determinations on three replicate analyses of SRM607 are similar to those of the Yemen samples, although Rb concentrations reproduce to only 0.9%. This propagates through to result in a Rb–Sr ratio reproducibility of ca. $\pm 0.4\%$. In this case, poor reproducibility can be attributed to sample heterogeneity, the relatively small amounts of this sample (ca. 10 mg) used in each analysis and relatively high isobaric interferences. In summary, we believe that the technique described herein allows us to measure Rb and Sr concentrations to ca. $< \pm 0.5\%$ and Rb–Sr ratios to $\leq \pm 0.2\%$ when the ^{87}Sr interference is two orders of magnitude less than the ^{87}Rb signal.

3.4. $^{87}Sr/^{86}Sr$ ratio reproducibility

Reproducibilities of $^{87}Sr/^{86}Sr$ ratios corrected for the presence of spike are presented in Table 3, again using either natural blank ratios or measured $^{87}Rb/^{85}Rb$ ratios from the Rb isotope dilution analysis to correct for isobaric interferences. In most cases, $^{87}Sr/^{86}Sr$ data corrected using natural Rb ratios give more consistent data than those corrected using measured ratios (e.g., NYJB140 and NYJB271). Reproducibilities for these ratios range from slightly to significantly worse than those gained for standard solutions and unspiked analyses of real samples by MC-ICPMS using identical procedures (0.003%; Waight et al., in preparation). In particular, Sr isotope ratios of the high Rb/Sr samples reproduce much more poorly. However, in the case of SRM607, reproducibilities (albeit for only three samples) for both $^{87}Rb/^{86}Sr$ and $^{87}Sr/^{86}Sr$ are significantly improved when the measured sample-spike $^{87}Rb/^{85}Rb$ and $^{87}Sr/^{86}Sr$ ratios are used for isobaric interference corrections. We attribute this sometimes significantly poorer reproducibility of $^{87}Sr/^{86}Sr$ for spiked samples to be a function of which $^{87}Rb/^{85}Rb$ ratio is chosen for isobaric corrections on ^{87}Sr, significant Rb interferences during the Sr analysis (e.g., NYJB232) and possible real sample heterogeneity in the case of the high Rb/Sr samples (which is ca. 27 Ma in age).

3.5. Rb–Sr geochronology

Geochronological results from the studied plutons are presented in Table 4. All ages are calculated using Isoplot (Ludwig, 1999) with $\lambda\ ^{87}Rb = 1.42 \times 10^{-11}\ a^{-1}$, and assigning 2 s.d. errors of 0.2% for $^{87}Rb/^{86}Sr$ (based on replicate analyses of whole rock powders and SRM607 with minimal isobaric interferences) and 0.003% for $^{87}Sr/^{86}Sr$, based on replicate analyses of SRM987 (Waight et al., in preparation), acknowledging that this may be an underestimate for Sr isotope analyses of spiked samples by MC-ICPMS. In some

Table 4
Geochronological results

Sample	Phase	Rb (ppm)	Sr (ppm)	$^{87}Rb/^{86}Sr$	$^{87}Sr/^{86}Sr \pm 2$ se[a]	Phases used	Age (Ma)[b]	$^{87}Sr/^{86}Sr_i$	MSWD
Jabal Hufash granite (Yemen)									
TW0040	kspr	183.4	24.26	22.11	0.71224 ± 2	ap–kspr	25.97 ± 0.11	0.70409 ± 2	
TW0041	amph	6.788	127.5	0.1539	0.70409 ± 2	amph–kspr	26.17 ± 0.11	0.70404 ± 2	
TW0042	ap	–	–	–	0.70409 ± 2	ap–amph–kspr	26.1 ± 1.9	0.7041 ± 3	12
Gardiner intrusion (East Greenland)									
TW0023	ap	–	–	–	0.70395 ± 2	cpx–bt	56.35 ± 0.24	0.70392 ± 2	
TW0043	bt	246.5	72.55	9.830	0.71179 ± 3	ap–bt	56.14 ± 0.24	0.70395 ± 2	
TW0044	cpx	3.439	958.0	0.0104	0.70393 ± 2	ap–cpx–bt	56.2 ± 2.4	0.70394 ± 19	3.9
Khibina carbonatite/apatite (Russia)[c]									
TW0034	ap	–	–	–	0.70338 ± 2	ap–bt(b)	366.4 ± 0.7	0.70338 ± 2	
TW0035	bt(b)	303.9	6.234	151.8	1.4952 ± 1	ap–bt(g)	364.4 ± 0.7	0.70338 ± 2	
TW0036	bt(g)	419.2	21.94	56.76	0.99805 ± 4	bt(1)–bt(2)	367.5 ± 1.2	0.701 ± 2	
						ap–bt(1)–bt(2)	366 ± 11	0.703 ± 1	15
Gouldsboro granite (ME, USA)									
TW0030	w.r.	60.28	282.6	0.6169	0.70817 ± 2	bt–w.r.	418.7 ± 0.9	0.70449 ± 3	
TW0031	plag	40.42	332.7	0.3513	0.70640 ± 2	bt–plag	420.2 ± 0.9	0.70430 ± 2	
TW0032	bt	226.5	70.54	9.333	0.76015 ± 2	bt–plag–w.r.	419 ± 17	0.7044 ± 12	136
Illimaussaq complex (South Greenland)									
TW0037	eud	–	–	–	0.71149 ± 2	eud–kspr	1160.1 ± 2.3	0.71149 ± 2	
TW0038	kspr	885.0	10.45	407.1	7.4727 ± 3	model kspr[d]	1161.2 ± 2.3	'0.70500 ± 2'	

Abbreviations: kspr = alkali feldspar, amph = amphibole, ap = apatite, bt = biotite (b = brown and g = green), cpx = clinopyroxene, w.r. = whole rock, plag = plagioclase and eud = eudialyte. MSWD = mean standard weighted deviation of isochron.

[a] Errors shown are 2 s.e. and represent either the stated reproducibility (0.003%), or the in run analytical error, whichever is largest.

[b] All ages were calculated using Ludwig's Isoplot v2.10a, using an assigned uncertainty (2 sigma absolute) of 0.2% for $^{87}Rb/^{86}Sr$ and errors given for $^{87}Sr/^{86}Sr$ in the table.

[c] Isobaric interferences for the Khibina Complex sample were corrected for using measured $^{87}Rb/^{85}Rb$ and $^{87}Sr/^{86}Sr$ ratios due to large Rb interferences during the Sr analysis. All remaining samples were corrected for isobaric interferences using natural ratios or assumed blank ($^{87}Rb/^{85}Rb = 0.3855$ and $^{87}Sr/^{86}Sr = 0.71$); see text for further discussion.

[d] Model age calculated assuming an initial $^{87}Sr/^{86}Sr$ of 0.7050 ± 2.

instances, the internal 2 s.e. of individual mineral analyses was larger than our external reproducibility (e.g., Sr isotopic analysis of Jabal Hufash apatite, where only a small amount of sample was collected). In these cases, the larger internal error is used in the age calculation.

There is generally an excellent agreement between previous age determinations on the investigated intrusions and the MC-ICPMS age data presented in Table 4. The calculated errors on the ages presented in Table 4 are around 0.4% of the absolute age for the young samples (Jabal Hufash and Gardiner) and around 0.2% absolute for the older samples. The effect of improved reproducibility of Rb–Sr ratios by this technique is most obvious in the older samples where there is sufficient range in $^{87}Sr/^{86}Sr$ such that the Rb–Sr ratio is the largest source of error in the isochron. The robustness of the Rb–Sr geochronological technique by MC-ICPMS is indicated by the fact that, where more than two phases have been analysed for an individual intrusion (i.e., Khibina, Jabal Hufash and Gardiner), calculated two-point isochrons internally agree within error. However, in most cases where more than two phases are available, the data failed to form statistically acceptable isochrons (i.e., MSWD>1.5).

Unlike other ages presented in Table 4, the Khibina carbonatite age was calculated using measured $^{85}Rb/^{87}Rb$ and $^{87}Sr/^{86}Sr$ ratios rather than natural values to correct for isobaric interferences. If natural values are used, this sample fails to form an isochron, yielding a meaningless age of ca. 500 ± 700 Ma. This

is a direct consequence of imperfect chemistry and relatively large Rb isobaric interferences during the two biotite Sr analyses, combined with their highly radiogenic compositions. For example, the 3.6% ^{87}Rb on ^{87}Sr interference during the TW0035 analysis results in a ~20% shift in the unmixed ^{87}Sr/^{86}Sr ratio from 1.8534 using natural ratios, to 1.4952 using measured ratios. In this case, using measured ratios to correct for isobaric interferences results in an age that is in agreement with previous age determinations. However, we emphasise that the true ratio for isobaric interference corrections must in fact be some mixture between sample, spike and blank and therefore, the age presented in Table 4 must be considered as an estimate only.

4. Discussion

4.1. Relative fractionation behaviour of Rb and Zr

Using mass fractionation of the ^{90}Zr/^{91}Zr ratio to correct the ^{87}Rb/^{85}Rb ratio assumes that the two elements fractionate identically during MC-ICPMS analysis. However, Rb and Zr are very different elements with distinct ionic charge and radii, Rb being a divalent large ion lithophile element whereas Zr is a tetravalent high field strength element. Where other element pairs have been examined in detail (e.g., Cu–Zn, Maréchal et al., 1999; Pb–Tl, White et al., 2000; Thirlwall, 2000), the assumption of identical and consistent behaviour during MC-ICPMS analysis has been observed to be less than ideal, although relative changes are less than 500 ppm. Therefore, before examining the reproducibility of our replicate standard and sample analyses and geochronological data, we examine the assumption of identical and consistent fractionation of Rb and Zr.

If Rb and Zr behave identically (i.e., have the same fractionation coefficients) during plasma ionisation then, following White et al. (2000) and Maréchal et al. (1999), the natural logs of fractionation uncorrected ^{87}Rb/^{85}Rb and ^{90}Zr/^{91}Zr should fall along a straight line defined by the relative atomic masses of the relevant isotopes (in this case a line with slope = −2.01 and intercept = 2.246). Plots of ln ^{87}Rb/^{85}Rb versus ln ^{90}Zr/^{91}Zr for standard solutions are presented in Fig. 4 and show that the two elements do not behave ideally (i.e., they have differing fractionation coefficients). Furthermore, the two elements appear to have different fractionation behaviours depending on the introduction system used (Micromist, Aridus, free aspiration, peristaltic pump, etc.). In particular, a small shift can be noted between the data collected in July 2000 using the Micromist 50 μl/min nebuliser and those collected in August 2000 using a Micromist 100 μl/min nebuliser, although the average values are the same within error (Fig. 1). It is important to note that tuning parameters (gas flows, torch position, etc.) were near identical during both these analytical sessions, therefore, the differences in fractionation of the two elements are not a consequence of instrument set-up.

Studies comparing fractionation of similar mass elements (e.g., Maréchal et al., 1999) have argued that most isotopic fractionation during plasma source spectrometry occurs in the plasma. We also suggest that the differing fractionation behaviour of Rb and Zr observed also reflects differing behaviour of elements in the plasma, due to the differing properties (principally wetness) the sample introduction systems impart to the solutions and the effects this has on the Ar plasma. The Aridus desolvating nebuliser introduces a largely dry sample into the plasma, whereas the 50-μl/min nebuliser produces a relatively wet solution and the 100-μl/min nebuliser an even wetter solution. Differing amounts of liquid in the sample solution entering the plasma will affect the plasma temperature and vary space charge effects, therefore changing the ionisation efficiency of the Ar plasma and the relative fractionation of Rb and Zr. What is vital to note is that the relative differences in fractionation between Rb and Zr indicated in Fig. 4 are insignificant compared to the level of precision required for an isotope dilution measurement. Even without restricting Rb isotope dilution analyses to a consistent sample introduction routine, the external reproducibility of all our standard Rb analyses is $\leq \pm 0.05\%$ (Fig. 1).

4.2. Reproducibility and accuracy of Rb concentration and Rb–Sr ratio determinations in solution, rock and mineral standards

Repeated analysis of natural Rb admixed with Zr suggests that the mass fractionation corrected Rb isotope ratio can be readily measured to ca. 0.05%

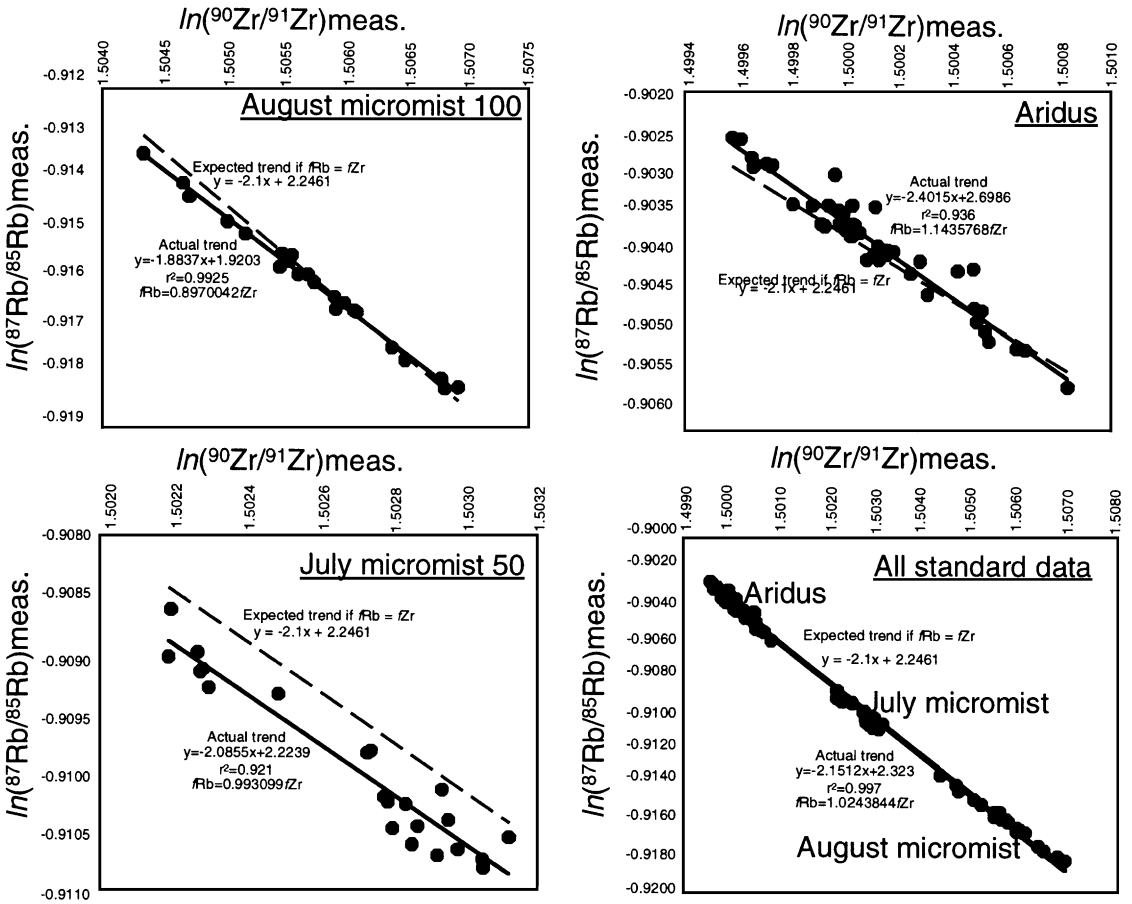

Fig. 4. Plots of ln $^{87}Rb/^{85}Rb$ versus ln $^{90}Zr/^{91}Zr$ for different analysis periods and different sample introduction systems. Dashed lines represent expected data trend if Rb and Zr behaved identically. Solid line represents calculated best fit line through each data set.

(Fig. 1). Therefore, in principal, Rb concentrations of real samples should also be measurable to these levels of reproducibility if:

1. twenty nanograms of Rb are available for analysis and the sample is not seriously under- or over-spiked resulting in error magnification on calculated Rb concentrations;
2. matrix elements remaining from chemical separation do not cause changes in relative fractionation of Rb and Zr, or result in unaccounted for isobaric interferences on masses 85, 87, 88, 90 or 91;
3. the samples are homogeneous;
4. weighing errors can be minimised.

In reality, our results show that Rb (and Sr) concentration determinations are an order of magnitude worse than that suggested by standard solution data. However, this remains a very acceptable reproducibility for elemental concentration determinations and the scatter is mostly a consequence of weighing errors, sample heterogeneity and imperfect chemical separation of Rb and Sr. In contrast to concentration determinations, the use of a mixed spike minimises propagation of weighing errors into Rb–Sr ratio determinations, therefore much of the scatter in these measurements must be derived from sample heterogeneity and imperfect corrections for isobaric interferences. For example, we attribute the poor Rb–Sr ratio reproducibility for sample (NYJB140, $\pm 0.5\%$) to

either sample heterogeneity or, more likely, the persistent and relatively high Sr interferences present on the Rb cut and the uncertainty as to which Sr ratio to adopt for correction of the isobaric interference on ^{87}Rb. Reproducibility of Rb–Sr ratios measured on three replicate analyses of SRM607 are similar to that of the low Rb/Sr sample ($\pm$ 0.5%). However, in this case we attribute this poor reproducibility to sample heterogeneity and the relatively small amounts of this sample (ca. 10 mg) used in each analysis.

The uncertainty as to which Sr isotope ratio to use to correct for isobaric interferences of ^{87}Sr during a Rb analysis can be directly attributed to imperfect separation of Rb and Sr during column chemistry. If a good separation of the two elements is achieved, then the isotopic composition of Sr interfering during the Rb analysis will be dominated by natural or environmental blank compositions. Furthermore, the relatively low interference results in considerably more flexibility in the composition to be used to correct for isobaric interferences (the same is true for Sr analyses). In contrast, a relatively large isobaric interference (several percent) is indicative of imperfect separation of Rb from Sr and therefore, the measured spiked sample ^{87}Sr/^{86}Sr ratio is more appropriate for interference correction during the Rb analysis. In reality, the interfering isotopic composition will be somewhere between a blank composition and that measured on the spiked Sr cut. Uncertainties in the exact ratio of this mixture will affect the accuracy of individual measurements. Therefore, we stress the importance of good chemical separations to yield accurate Rb concentration data and reproducibilities for Rb–Sr ratio determinations of $\pm$ 0.2% or better.

4.3. Reproducibility of $^{87}Sr/^{86}Sr$

Measurement of ^{87}Sr/^{86}Sr ratios by MC-ICPMS will be discussed in more detail in a separate contribution (Waight et al., in preparation), however, analysis of spiked Sr isotope analyses by MC-ICPMS is worthy of limited discussion here. The effects of isobaric interferences of ^{87}Rb on ^{87}Sr are magnified when it comes to determining Sr isotopic compositions on spiked samples, and this is reflected in the poor reproducibility for ^{87}Sr/^{86}Sr in several samples presented in Table 3. Our data suggest that ^{87}Rb/^{87}Sr needs to be on the order of $<$0.01% to yield good quality Sr isotope determinations. The arguments presented above for the need for good chemical separations of Rb and Sr, and the problematic issue of which ^{87}Rb/^{85}Rb composition (natural or measured) to use for correcting for isobaric interferences if they are high are even more applicable to Sr.

One important conclusion of this study is that Sr isotope analysis of spiked samples by MC-ICPMS is disadvantaged compared to TIMS analysis due to the similar ionisation efficiencies of Rb and Sr. This means that by MC-ICPMS, it is not possible to directly measure the isotopic composition of the Rb present in the Sr cut (without Sr interferences), whereas by TIMS this is feasible at low temperatures prior to Sr ionisation, allowing for more accurate internal interference corrections. Furthermore, during MC-ICPMS analysis, Rb and Sr ionise at the same efficiency, whereas Rb is 'burnt off' from the Sr cut during TIMS analysis (due to lower ionisation temperatures), significantly minimising the effect of isobaric interferences. However, it should be noted that during TIMS analyses, any Rb which is present may be highly fractionated and changing in composition during the analysis, making corrections for isobaric Rb on Sr far from straightforward. Splitting and spiking samples for separate Rb–Sr isotope dilution and isotopic composition analyses would improve ^{87}Sr/ ^{86}Sr determinations by MC-ICPMS, however, in general, we would recommend that spiked Sr isotopic analyses for geochronology are measured by TIMS. This limitation does not effect our estimate of the reproducibility of the Rb–Sr ratio measurement ($\pm$ 0.2%) by this technique. Moreover, examples of Rb–Sr dating presented here suggest that at least part of the degradation of Sr isotope reproducibility is a function of heterogeneity (JB232 and SRM607) as the calculated ages show good agreement with previous age determinations. An improvement in Sr isotope ratio determinations by MC-ICPMS is likely if a mixed spike constructed from ^{85}Rb and double pass Sr (99.6% ^{84}Sr) was used, reducing isobaric interferences at mass 87 and reducing errors generated by uncertainties in spike composition during unmixing calculations.

4.4. Rb–Sr geochronology

Our examples of Rb–Sr dating produces ages that are consistent with previous age determinations by a

number of methods in diverse samples ranging in ages from 25 to 1160 Ma (Table 4). For example, our Rb–Sr age for the Illimaussaq intrusion is identical (and has comparable errors) to a U–Pb baddelyite age from the same intrusion (Markl., personal communication). Small discrepancies between $^{40}Ar-^{39}Ar$ ages for the Gardiner complex and the Rb–Sr ages presented here may simply be a consequence of imperfect age constraints for the monitor mineral used during Ar dating. Uncertainties on calculated two-point Rb–Sr ages using our proposed reproducibilities are ca. $< \pm 1-3$ Ma in samples with ages of 365–1160 Ma (ca. 0.2%). The younger Yemen and Greenland samples lack the Sr isotope contrast between the low and high Rb/Sr phases to make full use of the improved Rb/Sr determinations made by MC-ICPMS and have age errors which are only 0.4%. In the case of the older plutonic rocks where different mineral phases permit calculation of several two-point isochrons, calculated ages also agree to within error, again testifying to the reproducibility of the technique.

Where three or more phases are present, our data fails to form statistically acceptable isochrons with MSWD's less than 2.5. This may be in part due to an overestimation of the reproducibility for $^{87}Sr/^{86}Sr$ ratios, which we have shown to be problematic by MC-ICPMS, or a consequence of small errors in the calibration of our different Rb–Sr spikes. However, some of the scatter on three-point isochrons may in fact be due to real geological scatter and a result of the reliance on apatite to constrain an initial $^{87}Sr/^{86}Sr$ composition. In the presence of highly radiogenic phases such as biotite (e.g., Khibina) or alkali feldspar (e.g., Yemen and Ilimaussaq), coexisting apatite may absorb loosely held radiogenic ^{87}Sr (particularly in the presence of fluids) and subsequently fail to fall on an isochron with other phases (Fig. 5). This would result in two-point isochron ages calculated using apatite and lower Rb/Sr minerals being lower than those calculated for apatite and the higher Rb/Sr minerals in the same samples (Fig. 4). Such an effect is most obvious in the Khibina sample where there is a wide range in Rb/Sr and $^{87}Sr/^{86}Sr$ to amplify the effect, but the fact that consistent patterns are observed in the two other samples where apatite is used to constrain initial $^{87}Sr/^{86}Sr$ indicate this is a real geological phenomenon, however, it would not be discernable

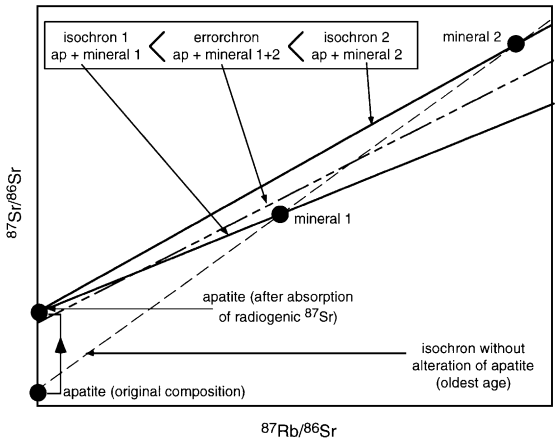

Fig. 5. Schematic diagram (highly exaggerated) showing the effects of addition of radiogenic ^{87}Sr to apatite to calculated two-point and three-point isochrons. The real age of the unit (thin dashed line defined by original isotopic composition of apatite) will only be revealed by a two-point isochron not involving apatite (mineral 1 + mineral 2). Using the most radiogenic mineral and apatite yields the age closest to the real age, and the relatively radiogenic apatite means the three minerals fail to form an isochron. The same age variations can be observed in all our isochrons, which use apatite to constrain the initial $^{87}Sr/^{86}Sr$ composition.

using TIMS data with errors of 1%. A similar effect could be attributed to the presence of Rb in apatite and radiogenic in-growth (all our apatites are analysed unspiked), however bulk analyses of our apatite samples show their Rb contents to be negligible ($^{87}Rb/^{86}Sr < 0.0001$).

4.5. Implications for Rb–Sr geochronology

We have presented a new technique for the measurement of Rb concentration data and Rb–Sr ratios where mass fractionation of the Rb isotope system during analysis is monitored using a stable Zr isotope ratio. The method enables determination of Rb–Sr ratios to $\leq 0.2\%$ providing a clean Rb cut is produced for analysis. The additional Rb clean-up step required for MC-ICPMS analysis is not a significant amount of work given the time (and cost) involved in making and degassing filaments for TIMS Rb analysis. Furthermore, the levels of reproducibility by MC-ICPMS represent a significant improvement over likely estimates of reproducibility on Rb–Sr ratios determined by TIMS analysis (ca.

1%). Measurement of Rb by MC-ICPMS isotope dilution should thus permit:

(1) significantly improved Rb–Sr age determination on samples from radiogenic systems where there is sufficient isotopic contrast (i.e. $\Delta^{87}Sr/^{86}Sr \geq 0.1$) to make the uncertainty on the Rb–Sr ratio the principal source of error;

(2) more detailed and reliable information from the Rb–Sr geochronological technique to be integrated with other (e.g., $^{40}Ar/^{39}Ar$ and U–Pb) age determinations in older suites of rocks, particularly with respect to the thermal history of the lithosphere;

(3) improved Rb/Sr determinations and geochronology on much smaller samples (e.g., sub-milligram mica crystals or micro-drill samples) for analysis by MC-ICPMS, only ca. 20 ng of Rb is required for a good quality Rb analysis and small Sr samples can easily be analysed by TIMS by loading on Re or W filaments with a TaF or TaCl activator;

(4) a reevaluation of the ^{87}Rb decay constant, which will be essential if point (2) is to exploited. In a recent summary, Begemann et al. (2001) observed that the decay constant for Rb (1.42×10^{-11} a^{-1}) recommended by Steiger and Jäger (1977) is poorly constrained and may in fact be 1–3% too high, they subsequently call for a redetermination of λ_{87}. This can be done by comparison of Rb–Sr ages with ages determined by other techniques on preferably relatively old and quickly cooled units. However, for such an investigation to be successful, accurate calibration of mixed Rb–Sr spikes and, to a lesser extent, consensus over the true Zr isotopic composition will be necessary.

5. Conclusions

We have developed a technique that uses Zr to correct for mass fractionation observed during isotope dilution analyses of Rb by MC-ICPMS. This technique consumes only ca. 20 ng of Rb and allows Rb–Sr ratios to be determined to $\leq 0.2\%$ when Sr is effectively separated from Rb, which is at least a factor of five improvement over Rb isotope dilution analyses by TIMS where mass fractionation of Rb cannot be readily controlled or monitored. This is confirmed by duplicate analyses of natural Rb standards and spiked mineral samples which clearly show much poorer data quality by TIMS than by MC-ICPMS. A typical MC-ICPMS analysis lasts only a few minutes and most of this time is devoted to sample washout.

Complications with the technique arise from the isobaric interference of ^{87}Sr on ^{87}Rb (and vice versa), and the similar ionisation efficiencies of the two elements by MC-ICPMS. When a good separation of Rb and Sr is achieved, these isobaric interferences are minimised and can be efficiently corrected using natural ratios, indicating that the interference is dominated by environmental blank. Given the complications of correcting for Rb isobaric interferences during spiked Sr isotope analyses by MC-ICPMS, it may be advantageous to carry out such Sr isotopic ratio analyses (particularly small samples) by TIMS where Rb interferences are effectively removed by the higher temperatures of Sr ionisation compared to Rb, or Rb can be measured prior to Sr ionisation. Application of the technique to a series of intrusions ranging in age from 26 to 1160 Ma has yielded results, which are in good agreement with previous age determinations.

Application of this technique will enable: (1) improved Rb–Sr dating of older rocks where precision and accuracy of the $^{87}Rb/^{86}Sr$ ratio is the major source of error; (2) greater confidence in the use of Rb–Sr system in constructing thermal histories of the lithosphere in conjunction with other thermochronometers and; (3) revolutionary application of Rb–Sr mineral dating to micro-samples. A reevaluation of the Rb decay constant is urgently needed to take advantage of some of the potential improvements in Rb concentration determinations. Comparison of Rb–Sr ages determined by our technique on a simple, rapidly cooled igneous sample which can be precisely dated by other isotopic systems (U–Pb, Lu–Hf and ^{40}Ar–^{39}Ar) would represent an important first step in this regard.

Acknowledgements

We thank Kent Brooks and Troels Nielsen who kindly supplied samples of the Illimaussaq, Gardiner and Khibina intrusions, and Bob Wiebe who provided the Gouldsboro granite sample. The people at TJA solutions/ThermoElemental, in particular Steve Guilfoyle are thanked for their support and advice with the operation of the Axiom. Dave Peate and Eirik

Krogstad assisted with discussions on laboratory protocol, analytical problems and technique development in the DLC MC-ICPMS laboratory. K. Ludwig and T. Hirata provided helpful reviews, which improved the clarity of the manuscript. M. Bickle is thanked for editorial comments.

References

Anbar, A.D., Roe, J.E., Barling, J., Nealson, K.H., 2000. Nonbiological fractionation of iron isotopes. Science 288, 126–128.

Bailey, J.C., Larsen, L.M., Sørensen, H., 1981. The Ilímaussaq intrusion, South Greenland: a progress report on geology, mineralogy, geochemistry and economic geology. Grøn. Geol. Unders., Rapp. 103, 130 pp.

Baker, J.A., 1996. Stratigraphy, geochronology and geochemistry of Cenozoic volcanism in western Yemen. PhD thesis, Royal Holloway University of London, 385 pp.

Baker, J., Snee, L., Menzies, M., 1996a. A brief Oligocene period of flood volcanism in Yemen: implications for the duration and rate of continental flood volcanism at the Afro–Arabian triple junction. Earth Planet. Sci. Lett. 138, 39–55.

Baker, J.A., Thirlwall, M.F., Menzies, M.A., 1996b. Sr–Nd–Pb isotopic and trace element evidence for crustal contamination of plume-derived flood basalts: Oligocene flood volcanism in western Yemen. Geochim. Cosmochim. Acta 60, 2559–2581.

Begemann, F., Ludwig, K.R., Lugmair, G.W., Min, K., Nyquist, L.E., Patchett, P.J., Renne, P.R., Shih, C.Y., Villa, I.M., Walker, R.J., 2001. Call for an improved set of decay constants for geochronological use. Geochim. Cosmochim. Acta 65, 111–121.

Blaxland, A.B., van Breemen, O., Emeleus, C.H., Anderson, J.G., 1976. Age and origin of agpaitic magmatism at Ilímaussaq, South Greenland: Rb–Sr study. Lithos 9, 31–38.

Blichert-Toft, J., Chauvel, C., Albarede, F., 1997. Separation of Hf and Lu for high-precision isotope analysis of rock samples by magnetic sector multiple collector ICP-MS. Contrib. Mineral. Petrol. 127, 248–260.

Capaldi, G., Chiesa, S., Manetti, P., Orsi, G., Poli, G., 1987. Tertiary anorogenic granites of the western border of the Yemen Plateau. Lithos 20, 433–444.

Coleman, R.G., DeBari, S., Peterman, Z., 1992. A-type granite and the Red Sea opening. Tectonophysics 204, 27–40.

Gleadow, A.J.W., Brooks, C.K., 1979. Fission track dating, thermal histories and tectonics of igneous intrusions in East Greenland. Contrib. Mineral. Petrol. 71, 45–60.

Halliday, A.N., Lee, D.-C., Christensen, J.N., Rehkamper, M., Yi, W., Luo, X.Z., Hall, C.M., Ballentine, C.J., Pettke, T., Stirling, C., 1998. Applications of multiple collector-ICPMS to cosmochemistry, geochemistry and paleoceanography. Geochim. Cosmochim. Acta 62, 919–940.

Hirata, T., Yamaguchi, T., 1999. Isotopic analysis of zirconium using enhanced sensitivity-laser-ablation-multiple collector-inductively coupled mass spectrometry. J. Anal. At. Spectrom. 14, 1455–1459.

Kramm, U., Kogarko, L.N., Kononova, V.A., Vartiainen, H., 1993. The Kola alkaline province of the CIS and Finland: precise Rb–Sr ages define 380–360 Ma age range for all magmatism. Lithos 30, 33–44.

Ludwig, K.R., 1999. Isoplot version 2.10a. Berkeley Geochronology Centre Special Publication 1.

Maréchal, C.L., Télouk, P., Albarède, F., 1999. Precise analysis of copper and zinc isotopic compositions by plasma-source mass spectrometry. Chem. Geol. 156, 251–273.

Minster, J.F., Ricard, L.P., 1981. The isotopic composition of zirconium. Int. J. Mass Spectrom. Ion Phys. 37, 259–272.

Nielsen, T.F.D., 1981. The ultramafic cumulate series, Gardiner Complex, East Greenland. Contrib. Mineral. Petrol. 76, 60–72.

Nielsen, T.F.D., Buchardt, B., 1985. Sr–C–O isotopes in nepehelintic rocks and carbonatites, Gardiner Complex, Tertiary of East Greenland. Chem. Geol. 53, 207–217.

Nielsen, T.F.D., Holm, P.M., 1993. Nd and Sr isotope compositions from the Gardiner Complex, East Greenland Tertiary igneous province. Bull. Geol. Soc. Den. 40, 280–287.

Nielsen, T.F.D., Solovova, I.P., Veksler, I.V., 1997. Parental melts of melilitolite and origin of alkaline carbonatite: evidence from crystallised melt inclusions, Gardiner complex. Contrib. Mineral. Petrol. 126, 331–344.

Nomura, M., Kogure, K., Okamoto, M., 1983. Isotopic abundance ratios and atomic weight of zirconium. Int. J. Mass Spectrom. Ion Phys. 50, 219.

Paslick, C.R., Halliday, A.N., Davies, G.R., Mezger, K., Upton, B.G.J., 1993. Timing of Proterozoic magmatism in the Gardar province, southern Greenland. Bull. Geol. Soc. Am. 105, 272–278.

Sahoo, S.K., Masuda, A., 1997. Precise measurement of zirconium isotopes by thermal ionization mass spectrometry. Chem. Geol. 141, 117–126.

Sanloup, C., Blichert-Toft, J., Telouk, P., Gillet, P., Alberede, F., 2000. Zr isotope anomalies in chondrites and the presence of ^{92}Nb in the early solar system. Earth Planet. Sci. Lett. 184, 75–81.

Steiger, R.H., Jäger, E., 1977. Subcommision on geochronology: convention on the use of decay constants in geo- and cosmochronology. Earth Planet. Sci. Lett. 36, 359–362.

Stevenson, R., Upton, B.G.J., Steenfelt, A., 1997. Crust–mantle interaction in the evolution of the Ilímaussaq Complex, South Greenland: Nd isotope studies. Lithos 40, 189–202.

Stirling, C.H., Lee, D.C., Christensen, J.N., Halliday, A.N., 2000. High-precision in situ U-238–U-234–Th-230 isotopic analysis using laser ablation multiple-collecter ICPMS. Geochim. Cosmochim. Acta 64, 3737–3750.

Thirlwall, M.F., 2000. Precise Pb isotope analysis of standards and samples using an Isoprobe multicollector ICPMS: comparisons with double spike thermal ionisation data. J. Conf. Abstr. 5, 996.

Tommasini, S., Poli, G., Manetti, P., Conticelli, S., 1994. Oligo–Miocene A-type granites and granophyres from Yemen: isotopic and trace element constraints bearing on their genesis. Eur. J. Mineral. 6, 571–590.

Upton, B.G.J., Emeleus, C.H., 1987. Mid-Proterozoic alkaline magmatism in southern Greenland: Gardar Province. In: Fitton, F.G., Upton, B.G.J. (Eds.), Alkaline Igneous Rocks, vol. 30. Geol. Soc. Spec. Publ., London, pp. 449–471.

Vance, D., Thirwall, M., 2000. Precise and accurate Neodymium

isotopic analysis of sub-5 ng samples by MC-ICPMS. J. Conf. Abstr. 5, 1042.

Walder, A.J., Freeman, P.A., 1992. Isotope ratio measurement using a double-focusing magnetic source mass analyser with an inductively coupled plasma as an ion source. J. Anal. At. Spectrom. 7, 571–575.

Walder, A.J., Furuta, N., 1993. High-precision lead isotope ratio measurement by inductively coupled plasma multiple collector mass spectrometry. Anal. Sci. 9, 675–680.

White, W.M., Albarède, F., Télouk, P., 2000. High-precision analysis of Pb isotope ratios by multi-collector ICP–MS. Chem. Geol. 168, 257–270.

Wiebe, R.A., Adams, S.D., 1997. Felsic enclave swarms in the Gouldsboro Granite, Coastal Maine: a record of eruption through the roof of a silicic magma chamber. J. Geol. 105, 617–627.

Wiebe, R.A., Ulrich, R., 1997. Origin of composite dikes in the Gouldsboro granite, coastal Maine. Lithos 40, 157–178.

Yi, W., Halliday, A.N., Lee, D.C., Rehkamper, M., 1998. Precise determination of cadmium, indium and tellurium using multiple collector ICP–MS. Geostand. Newsl. 22, 173–179.

Zhu, X.K., O'Nions, R.K., Guo, Y., Belshaw, N.S., Rickard, D., 2000. Determination of Cu isotope variation by plasma source mass spectrometry: implications for use as geochemical tracers. Chem. Geol. 163, 139–149.